

Magnetic Actuated Catheterization Robotics

Bok Seng Yeow and Ren Hongliang

Abstract This chapter covers the design principles of magnetic actuated catheter robot and is outlined as follows. Section 1 discusses key fundamental principles to design for an electromagnetic catheter/guide wire type surgical robot. The clinical perspectives are covered in Sect. 1.1 and in Sect. 1.2 the overarching electromagnetic theory is mentioned. Electromagnetic systems can be further decomposed into the stators (stationary wound coils) and actuators (moving part usually consists of permanent magnet), where the stators can be interpreted as the input and the actuator the output. Section 2 will cover the design consideration of stators and Sect. 4 the design principles of the actuators. Sections 2 and 3, aim to provide the reader with an intuitive approach to designing their own electromagnetic system. Section 3 will further exemplify principles covered in Sects. 2 and 3 with a fabricated prototype from our lab. These electromagnetic catheter systems can be classified by many parameters; one important parameter is the bending angle and will be addressed in Sect. 4. The use of this angle is demonstrated for a surgical context. This chapter concludes in Sect. 8, providing an overview of the works presented and the future directions.

1 Medical Background

1.1 AV Fistula

Arteriovenous fistula is a specific treatment support option for patients experiencing renal failure and requiring hemodialysis [24]. During dialysis, a machine replaces the patient's lost kidney function of blood filtration to prevent accumulation of toxic waste products [18]. During dialysis, the blood from the patient has to be rerouted into the machine and this requires venous access. There are other alternatives such as an access catheter or via grafts [54], fistulas allowing an increase in blood volumetric flux which is beneficial to the performance of the procedure. The increase in blood

B.S. Yeow · R. Hongliang (✉)

Department of Biomedical Engineering, National University of Singapore, Singapore, Singapore
e-mail: ren@nus.edu.sg

© Springer Nature Singapore Pte Ltd. 2018

H. Ren and J. Sun (eds.), *Electromagnetic Actuation and Sensing in Medical Robotics*,
Series in BioEngineering, https://doi.org/10.1007/978-981-10-6035-9_4

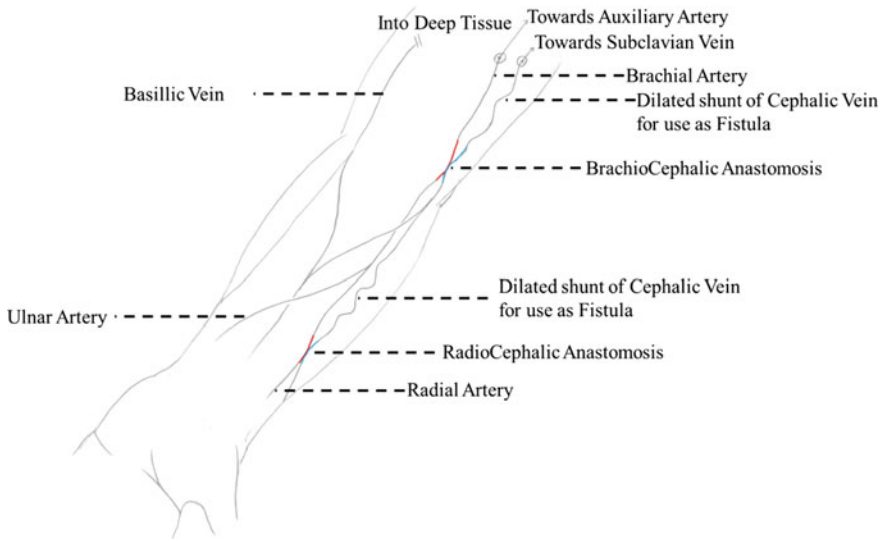


Fig. 1 Vasculature in the upper limbs.

flow comes from rerouting an artery to a vein which is connected via an anastomosis [24]. This causes the vein to build up pressure over time and will dilate. The enlarged vein acts as an easy access for dialysis and this technique can be applied to a wide variety of location. Common sites include the upper limbs using the Radial, Ulnar, Brachial and Cephalic [35], Fig. 1.

The connection technique between arteries and veins can vary depending on the situation such as transposition (the distal drainage network of a vein is replaced with flow from the artery) and interposition (flow from the arteries bifurcates into the vein via a graft connecting the two) [24].

1.2 Stenosis

Utilizing the fistulas overtime will develop into stenosis [1], as there is constant needle access [20, 53]. The constant needle access results in tissue trauma and develops scar tissue; furthermore, there could be fistula thrombosis [11]. These medical issues result in the reduction of volumetric blood flow [17] and should be reopened via angioplasty [25].

Angioplasty involves inserting a surgical balloon or stent into the lumen of the vessel, which expanded to increase the size of the lumen. To reduce surgical trauma and improve surgical success rates, it is common to access the target area via a distal access site. A guide wire is to create an access line connecting the distal access site to the target site. A catheter then run over the guide wire to replace the guide wire.

Surgical tools such as the surgical balloon then traversed through the catheter to reach the target site to carry out its functions.

1.3 Challenges and Benefits

In the less ideal and more likely scenario, there will be challenges in performing the procedure. In positioning of the guide wire under the guidance of angiography and ultrasound, visual acuity in trying to place the guide wire is lacking. Further, there is poor transmission of forces to the distal tip as control is mechanically initiated from the proximal end and is expected to traverse the entire insertion length. The transmission is easily compromised with tortuous environments where the guide wire easily buckles. Physicians utilize various shapes of guide wire [37] and handling techniques [26] to mitigate the current limitations in guide wires. The concepts described in the following chapters intend to provide physicians with a more direct control over the distal tip via electromagnetic coupling. The electromagnetic approach is more direct as the control information outside of the patient is not attenuated along the guide wire path.

1.4 Arteriovenous Fistulas and Electromagnetic Actuation

Minimally invasive surgeries [24] involve teleoperation of surgical equipment and are widely employed in vascular surgeries due to benefits, in patient recovery times, over open surgery [18]. Vascular surgeries typically involve guide wire placement prior to angioplasty (balloon or stent) procedures [54]. There exist a wide variety of vascular targets such as arteriovenous fistulas which are superficial veins/arteries at the dermal surface. This reduces constraints on the design of the system as the magnetic fields need not be as strong to penetrate and reach the deep vasculature. Arteriovenous fistulas are important to hemodialysis patients as access sites for renal therapy; in the 2011 Kidney Dialysis Foundation report, 76.6% of Singapore hemodialysis patients are reliant on arteriovenous fistula [35]. These fistulas, however, tend to close-up over time due to constant needle access [1, 35] inducing tissue trauma and developing stenosis [20]. Angioplasty remains an important surgical option for the management of stenosis in arteriovenous fistulas [53].

The guide wire has to traverse the length of the fistula, mediating across the stenosis. For our problem statement, we assume that complete total occlusion has not occurred. The surgeon is challenged by limited vision and control in the determination of guide wire positions during the navigation phase [11]. Surgeons have to be dexterous and experienced to not over exert pressure which can puncture the vasculature [11] and employ skilful buckling of the different types [17] of guidewires

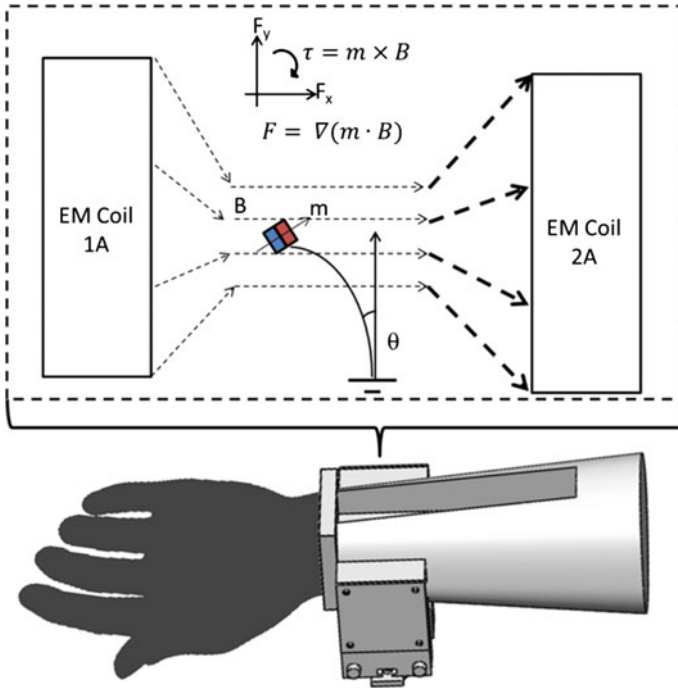


Fig. 2 Overview of the electromagnetic system.

to reach the correct destination. The challenges presented also vary between patient demographics [25] and the type of arteriovenous fistulas [37, 53]. In the case of overly torus routes [26], multiple stagings of catheters guide wires exchanges are needed, consuming time and resources.

Our system utilizes electromagnetic coil pairs that are configured near the stenosis site and defines the magnetic flux density at a region which is operator determined. When the guide wire is at the region of interest and the operator requires the guide wire to deflect in a particular manner (to check for guide wire advancement), the applied magnetic fields can be controllably changed. Changes in the applied magnetic fields interact with the magnetic attachment on the guide wire, inducing mechanical deflection of the guide wire, Fig. 2.

EM coil refers to the electromagnetic coils which generate the magnetic fields (represented by dotted arrows). The guide wire deflects an angle of θ due to interaction of the magnetic tip (red and blue box) in the magnetic field. The entire setup is orientated relative to the patient’s arm where tele-navigation of the stenosis is deemed necessary.

1.5 Overview and State of the Art

The use of electromagnetic manipulation systems can improve present surgical procedures [45, 55] despite reported risk from magnetic resonance heating [32]. Preexisting tetherless electromagnetic arts are classified here based on the actuator (Particle or Manipulator) or the stators (Electromagnetic coil). Arrangements [31, 33, 40] for the various stators, the control methodology of the magnetic navigation system [4, 6, 8, 10, 43, 47, 48] and the applications of the system [13, 46] can be defined separately. Publications associated with Stereotaxis [9, 21, 27, 36, 38, 39, 44, 49] or claiming novel actuators will be further considered due to the similarity in art.

Novel actuator ideas include converting the associated magnetic responsive elements in the manipulator, which is traditionally rigid, into a fluid [52], nanoparticles [12] or flexible magnets [16]. The magnetic component is also used to grab and advance other instruments [50]. Additional functionalities were associated with the navigation of the manipulator, such as with drilling tasks [5].

Comparing with guide wire actuator-based systems, magnetic micro-robot systems [3, 7, 19, 22, 23, 41] share similar operational mechanics to manipulator-based guide wires [2]. Tetherless magnetic control has also been used to couple the motion of a robotic arm to a magnetic capsule [31]. More recent setups include magnetic actuation of in-vivo cameras [30] or for high-frequency actuation such as in needless injectors [51].

Presently, the prototype holds much similarity in terms of methodology to designs claimed by Stereotaxis. The predetermined position of the magnetic element interacts with the external magnetic field enabling flexion. Our system differs from the above based on the applications to plaque navigation in fistulas and in the portability of the stator magnetic fields generators. Further, this prototype is preliminary and works toward the eventual disposable guide wire attachment for tetherless electromagnetic control. This will enable the angioplasty procedure to move into small clinics as the electromagnetic coils are much smaller and more portable. Additionally, the attachment will allow any type of guide wires to be controlled allowing ease of integration into hospitals.

1.6 Clinical Relevance (In Geographical Context)

Peripheral artery disease (PAD) has been indicated to be a growing problem [28] and is a type of atherosclerosis. In Singapore and many Asian countries, the risk factors associated with PAD are on the rise due to an unhealthy lifestyle and an increase in life expectancy [42]. PAD affects both the mortality and quality of lifestyle of patients and shares similar risk factors with other cardiovascular disease. Common methods for the diagnosis of PAD include the ankle brachial index [14] as PAD usually occurs in extremities of patients especially the lower limbs, affecting mobility. Surgical treatment such as atherectomy or angioplasty via stenting or balloon (US8348858,

US8419681) will require a guide wire to deliver the end effector to the desired location [15]. There are many types of catheter-guide wires configurations [34] for a wide range of purposes and control is challenging as complications may arise from perforations and buckling when using a distal controller. It is useful to define some functional definitions [34] of a guide wire.

(1) Wire trackability—is ease in which a wire can be advanced through a tortuous artery without buckling, kinking or prolapsing. This is related to the bend radius, arc length and number of bends of the artery which the guide wire has to traverse. This is similar to the dexterity requirements in the design of manipulators.

(2) Pushability—is the percentage of transmitted force from the shaft to the wire tip and relates to the axial and radial advancement of the guide wire.

(3) Penetration power—is the pressure that the tip can exert without buckling. This is essential when trying to penetrate through occlusions.

(4) Tactile response—is how the operator can comfortably and accurately control changes in movement of the wire tip.

(5) Tip load—quantifies the force to bend the distal tip of a wire. Stiffer wires are harder to bend and consequently easier to pierce through calcified/blocked arteries; but as they are stiffer, they require more force to bend and the forces exerted may cause puncture damage to the surrounding tissue. This is analogous to compliance in a manipulator.

There are further functional aspects of guide wire, which we will not consider as it is less related to the manipulability of the device durability, tip flexibility, tip malleability, etc.

2 Electromagnetic Principles in Magnetic Catheter Actuation

2.1 Magnetic Fields

All electromagnetic designs stem from Maxwell's equations which describe the coupling between electromagnetic fields as well as their spatial representations. While electric fields and magnetic fields are essentially carried by the same boson (photons), their oscillatory interactions with the human body are vastly different. Electric interactions are useful as sensors where the changes in electrical resistances and capacitance are detectable as in the case for ECG, EMG, EEG, etc. While magnetic fields have also been used for sensing (MRI), the magnetic fields required have to be very strong to pick up the atomic spin information. The human body is virtually invisible to weak magnetic fields and thus magnetic fields are a good choice for transmitting information into the body with minimal interference. The generations of magnetic fields are achieved artificially with an electric current which is characterized by Ampere's circuital law. The generated magnetic fields can then be used for subsequent actuation.

2.2 *Magnetic Circuit to Generate Magnetic Fields/Magnetomotive Force*

Much like Kirchoff's Law in electrical circuits, the magnetic circuits are the simplified law to model magnetics and are analogous to their electrical counterpart.

The electromagnetic coils (or wire winding/solenoid) act as magnetic dipole sources and generate the potential for magnetic fluxes. The flux density at the regions of interest can then be calculated by considering the integral over the total permeance/reluctances of paths.

The path considered for magnetic circuits can be challenging to define but it gives a good approximation to magnetic flux densities when the flux leakage of the source is small. This approach is best used when the air gap in consideration is small for the magnetic flux path in question. The consideration of the magnetic potential sources on the other hand is quite straight forward. Permanent magnets are characterized by their intrinsic magnetization values and act as fixed dipole sources. Solenoids or wound wires carrying current will generate magnetic fields and also act as magnetic sources. The following example demonstrates the calculations for the magnetic fields at any given point along the axis of a simple solenoid:

$$B = \frac{\mu_0 N I}{2} \int \frac{R^2 dx}{(x^2 + R^2)^{1.5}} \quad \text{where} \quad \left\{ \begin{array}{l} x = r \operatorname{ctg} \beta \\ dx = -R d\beta \frac{1}{\sin^2 \beta} \end{array} \right\} \quad (1)$$

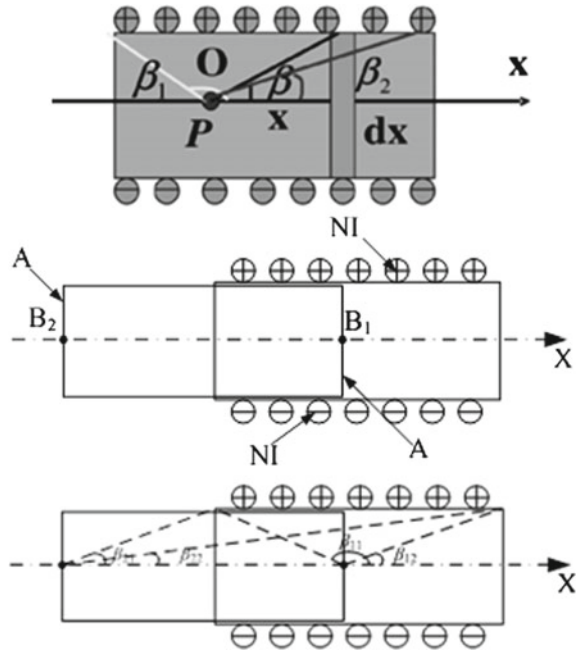
$$B = \frac{\mu_0 N I}{2} (\cos \beta_2 - \cos \beta_1), \quad (2)$$

where μ_0 is the permeability of free space, (H/m), and R (not in fig) is the radius of the solenoid (Fig. 3).

2.3 *Interpretation of Lorentz Forces*

This chapter considers the interactions between ferromagnetic materials in the generated magnetic fields. Two predominant models have been used in the calculation of forces between magnets (Magnetostatics): the Gilbert model and the ampere model. Finite-element models for the numerical derivation of magnetic force on ferromagnetic objects are commonly adopted for experiments handling complex geometries. The details of the Gilbert model and the Ampere model will not be discussed but rather the more general governing equations of (Eqs. (3) and (4)). The reader should still look up on the two models to check if their geometries fall under the classification of either the Gilbert or Ampere model assumptions, in which case the analysis can be simplified. Magnetic fields are controllable via current in electromagnetic coils, and the interaction between the applied magnetic field and a magnetized object is coupled by Lorentz forces which drive the mechanical actuation. By considering

Fig. 3 Models of solenoid.



magnetic dipole sources, the net actuation can be split into forces (F) and torques (τ):

$$F = V_{\text{volume}} (M \cdot \nabla) B \tag{3}$$

$$\tau = V_{\text{volume}} (M \times B) . \tag{4}$$

This actuation can be applied to a medical context for manipulating micro-robots, guide wires and catheters. The control over these instruments has a wide array of impact and below we discuss one such impact.

3 Magnetic Stators

3.1 Basic Coil Design

For the magnetic catheter to conduct information, there should be interaction between the external magnetic field generators and the magnetic element, which is inside the patient. For the general setup, the external electromagnetic coils are good targets for controller inputs.

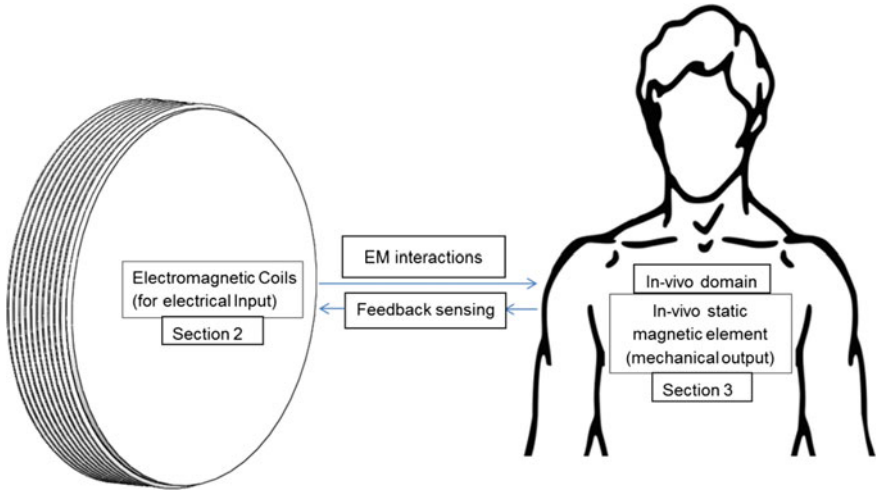


Fig. 4 Relative overview of actuator and stator in practice.

We begin with the design of electromagnetic coils which are the field generators. Varying currents in the EM coils will affect the eventual output position of the in-vivo magnetic elements. The simplest electromagnetic core consists of wound wires around a core material and can take on many designs depending on the requirements. The simplest design is a solid cylindrical core with wires winding coaxially around the core to form a cylindrical shell around the solid core (Fig. 4).

3.2 Electromagnetic Core Parameters

For a given solenoid, we define a region of interest where the generated magnetic fluxes from the solenoid change the magnetic field potentials and gradients for actuation. While it is possible to have an air core system (depending on the design and requirements), the currents may be high (resulting in heating concerns). Thus, incorporating a core material has benefits of concentrating magnetic fluxes and increasing magnetic field strengths at the region of interest. To further enhance the magnetic field, a closed flux path design is recommended to reduce the reluctance of the flux path as much as possible. This is achievable by encasing the solenoid in a magnetic permeable material, thus replacing the external air path with a more permeable material. Magnetic permeable materials will have a BH response curve which is important in the selection of materials [45].

BH curve shows the saturation/max operation for the material and is used to select the appropriate material for the purposes intended. Any material will have a response to the applied/surrounding magnetic fields; here, a magnetic field strength of \mathbf{H} is applied to the material and the magnetic field \mathbf{B} (synonymous the magnetic

flux density) in the material has a response characteristic to the material composition. Most materials have a saturation limit which should be above the design requirements to reduce losses. Other preferential aspects are the gradient of the operational region (such as optimized linearity, steepness), hysteresis loss (usually minimized via eddy loss minimization common in high-frequency operations) and other physical factors. The approach is to first solve for B field in the homogeneous region based on air coil design. Based on physical parameters for the coil, including I for current, L_{EM} for length, OD for outer diameter, ID for inner diameter, OD_{wire} for wire diameter and L_{wire} for wire length, we determine the turns per unit length (n):

$$r_{ave} = \frac{\frac{OD}{2} - \frac{ID}{2}}{2} + \frac{ID}{2} \quad (5)$$

$$N = \frac{L_{wire} \times 10^3}{2\pi \times r_{ave}} \times F \quad (6)$$

$$n = N \times \frac{L_{EM}}{OD_{wire}}. \quad (7)$$

The turn per unit length indicates the density of the coils and allows an estimation of the magnetic flux density at the centre of the solenoid (=1 for air core):

$$B = \mu_0 n I. \quad (8)$$

Next, the factoring of changes in the reluctances due to the magnetic permeable core.

B is related to H (magnetic field strength) and thus MMF (magnetomotive force F)

$$B = \mu H \quad (9)$$

$$F = \int H \cdot dl, \quad (10)$$

where dl refers to the flux path.

Depending on the cross-sectional area, flux density is usually the better parameter to describe the system as

$$\phi_B = \iint_s B \cdot ds, \quad (11)$$

which is the equation for describing the magnetic flux through a nominal surface S.

When using a soft magnetic core instead of an air coil, the reluctance (R_m) of the magnetic flux path is reduced:

$$\phi \cdot (R_m \downarrow) = (F \uparrow). \quad (12)$$

This will increase the perceivable magnetomotive force at the ROI, which is similar to the electric circuit. The changes to reluctance are determined experimentally to find a factor (μ_k) which changes the magnetic permeance (μ) of the flux path:

$$\mu = \mu_k \mu_0. \quad (13)$$

By relation to the above equations, the flux density is increased leading to the actuator perceiving stronger electromagnetic field for actuation.

To factor in the spatial position of the region of interest away from the coils, we utilize concepts covered in Sect. 2. The simplified and accessible approach to magnetic field state above does suffer from some limitations. The magnetic fields generated are in many cases not uniform but as EM coil area \gg permanent magnet/ROI, this is still a good approximation. However, if the field is nonuniform in the ROI, the above calculations will not be applicable such as when working near the electromagnetic coil surface. If so, alternative computational methods may be preferred.

From the general solenoid Eq. (2), I (current) and n (turns per unit length) are preferably maximized within the physical design limitations. The values of I and n are related inversely, and thus there exist an optimization between the values of n and I. To increase the number of turns, the wire diameter can be decreased:

$$\rho = R \frac{A}{L}. \quad (14)$$

The resistance is a function of the resistivity (R), material property and the geometrical relations of cross-sectional area (A) and length (L). Thin wires can increase the turns per unit length as the diameter of wires decreases and more wires can fit in the same area. However, this will reduce current as the cross-sectional area decreases (A) and resistance of the wire increases. An ideal case should optimize parameters for number of turns per unit length to desired current. This can be done experimentally or via simulation [55].

3.3 Geometrical Configuration

By varying the positions of coils, one can generate unique magnetic fields at the regions of interest. Each coil generates magnetic fields, and the summation of all these effects is translated into the eventual ROI fields. At higher frequencies and magnitudes, the signal can constructively or destructively interact with other coils which can be important to high-frequency and proximity designs. When considering design, start from the simplest level of actuation and move towards desired level of complexity. An example of magnetic translation can include 3 DOFs to translate a

permanent magnet in the X, Y and Z axis. We associate one coil pair to each degree of freedom (DOF). Thus, we would have three coil pairs one on each axis. Coil pairs are common in defining 1 DOF; however, this is not always necessary and a single coil is also capable of achieving the same. Coil pairs are, however, commonly used as the magnetic potential falls off greatly when moving away from the coil, and hence a much larger current is required. A coil pair counters this by having an opposite coil to maintain the field strengths. Having Helmholtz or Maxwell coil pairs will allow easier control over the well-modelled dipole field. The differences in input current between the two coils define the gradient and potential along that axis. In addition to field strengths, magnetic field uniformity at the region of interest is also preferred to improve ease of control. This relates to Sect. 3.2 where using a soft iron core which increases field strength will also make the magnetic fields less uniform.

3.4 Unique and More Novel Designs

While it is discussed above that coil pairs are coaxial to define a DOF, many other designs do not follow this. One example being OctoMag [15] which has eight electromagnetic coils but is unique in the layout to achieve 5 DOFs. OctoMag design in which four coils use opposite coil pair designs define the xy plane, while the other four coils rest above the other four coils to provide the additional z-plane motion. The control aspect of such a setup is very much more complicated and by this design 5 DOFs is achievable. Such a complex design is, however, well suited for ocular procedures where it would be difficult to place coils posterior to the eye. This is an example where the number of coil pair does not directly relate to the number of DOFs due to the design restrictions.

Most coils adopt a circular design to capture the symmetry in magnetic fluxes. However, coils need not always be circular; Square coils have been designed [40], and more complicated designs are possible depending on problem specifications. The physical assembly and arrangements of multiple coils (while individually symmetrical) can induce a loss of symmetry in the global system. Square coils can be designed to compensate for this and maintain the global symmetry in magnetic fields [33].

Other designs remove the need for an electromagnetic coil altogether. An actuator with 5 DOFs was achieved in [31] but utilized a single permanent magnet as a stator. Here, a robotic arm is used to provide the DOFs acting as the stator via a permanent magnet attached to the robotic arm. Magnetic forces are used to couple and transfer the position motion, and there are no electromagnetic coils used. The control, however, has to be closed loop, and depending on image feedback the robotic arm has to modulate the signals appropriately to control the positions of the actuator.

4 Magnetic Actuators

4.1 Magnetic Tip Attached to a Guide Wire Modelling

When the guide wire undergoes deformation due to energy input from the external coils, the increased energy state is balanced across the time frames. There are three energy domains for consideration in each time frame where the sum of the internal energies must equal to the energy state in the previous frame plus the energy change from the external system [47, 48]. The three energy domains are (1) magnetic potential energy, (2) strain energy and (3) contact deformation energy. A magnetic dipole in a nonuniform magnetic field will be displaced until it finds a stable low energy state; the energy it must seek out this minimum is the magnetic potential energy and is a result of the interactions between the magnetic field and the magnetic dipole. In our case of guide wire, the deflection in the tip will increase the strain energy in the guide wire. If the external forces acting to deflect the guide wire are interrupted, the strain energy in the guide wire will restore it to its neutral position. This strain energy can be modelled as a spring as a function of changes to neutral curvature or angular displacement. The contact deformation energy is more complex and is applicable to cases where the guide wire is in contact and is deforming a soft body, such as the walls of the vessel. This component can be a simple linear deformation or more complex viscoelastic Kelvin–Voigt deformation [4] and is dependent on the system in question. To keep the analysis, we consider only the magnetic potential energy in the following section.

4.2 Magnetic Forces and Torques on a Magnetic Dipole Point

Starting from the general equation, we reduce it depending on the system in question. For one-dimensional problems, consider a small permanent magnet (a magnetic dipole) moving on the coaxial axis (only B_y is nonzero, no M_z) between two electromagnetic coils.

The general force Eq. (15) and torque Eq. (16) equation can be reduced to one-dimensional Eqs. (17) and (18) in each component:

$$F = Volume (M \cdot \nabla) B \quad (15)$$

$$\tau = Volume (M \times B) \quad (16)$$

$$F_y = M_x \cdot \frac{dB_y}{dx} + M_y \cdot \frac{dB_y}{dy} \quad (17)$$

Table 1 The derivation of equations.

$\tau = \nabla(\vec{M} \times \vec{B})$	$F = \nabla(\vec{M} \cdot \nabla) \vec{B}$
$\begin{pmatrix} \tau_x \\ \tau_y \\ \tau_z \end{pmatrix} = \nabla \begin{pmatrix} M_y \cdot B_z - M_z \cdot B_y \\ M_z \cdot B_x - M_x \cdot B_z \\ M_x \cdot B_y - M_y \cdot B_x \end{pmatrix}$	$\begin{pmatrix} F_x \\ F_y \\ F_z \end{pmatrix} = \begin{pmatrix} M_x \cdot \frac{dB_x}{dx} + M_y \cdot \frac{dB_x}{dy} + M_z \cdot \frac{dB_x}{dz} \\ M_x \cdot \frac{dB_y}{dx} + M_y \cdot \frac{dB_y}{dy} + M_z \cdot \frac{dB_y}{dz} \\ M_x \cdot \frac{dB_z}{dx} + M_y \cdot \frac{dB_z}{dy} + M_z \cdot \frac{dB_z}{dz} \end{pmatrix}$
$\begin{pmatrix} \tau_x \\ \tau_y \\ \tau_z \end{pmatrix} = \begin{pmatrix} 0 \\ 0 \\ M_x \cdot B_y - 0^+ \end{pmatrix}$	$\begin{pmatrix} F_x \\ F_y \\ F_z \end{pmatrix} = \begin{pmatrix} M_x \cdot 0^+ + M_y \cdot 0^+ + 0 \\ M_x \cdot \frac{dB_y}{dx} + M_y \cdot \frac{dB_y}{dy} + 0 \\ 0 \end{pmatrix}$
$\tau_z = M_x \cdot B_y$	$F_y = M_x \cdot \frac{dB_y}{dx} + M_y \cdot \frac{dB_y}{dy}$

$$\tau_z = M_x \cdot B_y(x, y). \tag{18}$$

The derivation of Eqs. (15)–(18) is shown in Table 1.

There is no magnetization in Z or magnetic fields in the Z direction when considering motion in a 2D plane ($B_z = M_z = 0$). Note, however, the torque can exist in the Z plane as a consequence of the orthogonal vector convention. Further, there will not be any gradient variation in the Z direction when considering a 2D plane ($\frac{dB_z}{d(x,y)} = \frac{dB_{(x,y,z)}}{dz} = 0$).

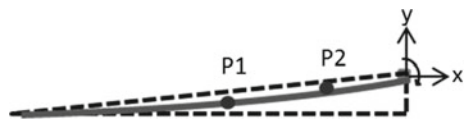
4.3 Application of Forces and Torques to a Cantilever Equation

By ignoring the strain energy and the contact energy, we can consider the system as a point-loaded cantilever. To consider the strain energy, the Young’s modulus can be replaced with a strain-dependent equivalent and contact deformation will include another considering term into the differential Eq. (18) (Fig. 5).

The Cantilever equation is given as

$$\frac{d^2y}{dx^2} = \frac{\iint \{F(x, y) < x - L >^{-1} - \tau(x, y) < x - L >^{-2}\}}{EI}. \tag{19}$$

Fig. 5 Relatively small angle deflection P1 & P2 of a modelled cantilever.



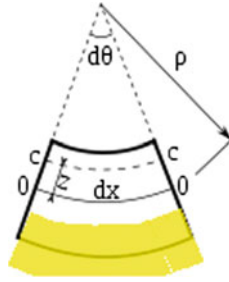


Fig. 6 Model of a bending segment.

For small angle approximations, the following relation holds:

$$\frac{dy}{dx} = \tan(\theta) \sim \theta \text{ rad.} \quad (20)$$

The curvature is then defined as

$$\frac{d\theta}{ds} = \frac{\text{angle - relative - to - origin}}{\text{position - along - curve}} = \frac{\theta(p2) - \theta(p1)}{s(2) - s(1)}. \quad (21)$$

The arc length is formulated by assuming that the plane sections remain plane after bending, where S is the arc length, R is the radius and is the angle in radians. Equation (21) is in differential form:

$$dS = R * d\theta. \quad (22)$$

The curvature is more commonly expressed as a function of the bending radius (Fig. 6),

$$\frac{d\theta}{ds} = \frac{1}{R}. \quad (23)$$

The length of the neutral axis (dx) is

$$dx = ds = \rho * d\theta. \quad (24)$$

Consider strain at the yellow region,

$$\epsilon = \frac{\Delta x}{x} = \frac{(\rho + z) \cdot d\theta - \rho \cdot d\theta}{\rho \cdot d\theta} = \frac{z}{\rho}. \quad (25)$$

For an isotropic material with young's Modulus E , the stress can be expressed as

$$\sigma = E\epsilon = E \frac{z}{\rho}. \quad (26)$$

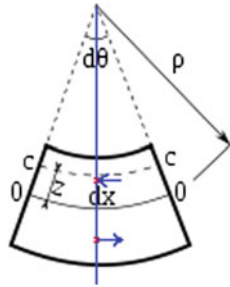


Fig. 7 Bending moment at dx.

Stress is also the force over an area. For this yellow portion, the forces are tensile, and strain is positive:

$$dF = E \frac{z}{\rho} dA. \tag{27}$$

For the opposite side, it will be in compression and we can couple both forces into a moment (Fig. 7).

The bending moment is

$$dM = dF \times z. \tag{28}$$

Substituting Eq. (26) into Eq. (27),

$$dM = E \frac{z^2}{\rho} dA. \tag{29}$$

The integration of Eq. (28) over the area is commonly expressed as

$$\frac{1}{\rho} = \frac{M}{EI}, \tag{30}$$

where I is known as the second moment of area and is the same as R in Eq. (22). Using Eqs. (19), (22) and (29), we can get the beam bending equation:

$$\frac{d^2y}{dx^2} = \frac{M}{EI}. \tag{31}$$

Depending on sign convention, the moment is sometimes written as $-M$. To solve the equation, we need the support or displacement boundary conditions are used to fix values of displacement (y) and rotations (dy/dx) on the boundary. Such boundary conditions are also called Dirichlet boundary conditions. Load and moment boundary conditions involve higher derivatives of y and represent momentum flux. Flux boundary conditions are also called Neumann boundary conditions.

Shear forces are related to bending moments by

$$\frac{dM}{dx} = -F. \tag{32}$$

A differential load $q(x)$ at a point can be expressed as

$$q(x) = -\frac{dF}{dx} = \frac{d^2M}{dx^2}. \tag{33}$$

Substituting Eqs. (31) and (32) into Eq. (30), we get

$$EI \frac{d^4y}{dx^4} = q(x), \tag{34}$$

which can be solved for a point-loaded cantilever with a tip load P :

$$y = -\frac{PL^3}{3EI}. \tag{35}$$

We can also use singularity functions to represent loadings. Singularity functions are indicated with angled brackets $\langle \rangle$ in contrast to traditional curved brackets $()$. Singularity function differentiates and integrates normally as one would with a standard variable (integrating $\langle x \rangle^2$ would give us $\frac{1}{3}x^3$) but the unique thing about singularity functions is that if the power is less than 0, we simply ignore the variable ($\int \langle x \rangle^{-2} = \frac{-1}{2} \langle x \rangle^{-1} = 0$ but will be apparent to higher degrees of integration). It is also similar to the unit step function in which if the evaluation in between the brackets is less than 0, the term is zero, and it is the variable if it is more than 0, i.e. ($\langle x - a \rangle^2 = 0$ for $x < a$, and $\langle x - a \rangle^2 = x^2$ for $x > a$).

(i) Constant load such that the load at m is ω_0 when $L > m > a$:

$$Load(m) = -\omega_0 \langle m - a \rangle^0 N. \tag{36}$$

(ii) Linear load such that the load at m is $b^*(m-a)$ when $L > m > a$. $\langle x - a \rangle^n$ and n can take on higher orders (Fig. 8):

$$Load(m) = b \langle m - a \rangle^1 N. \tag{37}$$

(iii) Moment load such that the load at m is M_0 when $L > m > a$. $\langle x - a \rangle^n$ After each integration, the value of n increases by 1, and thus the moment load is perceived only after two integrations (Fig. 9):

$$Load(m) = M_0 \langle x - a \rangle^{-2} N. \tag{38}$$

(iv) Impulse load such that the load at m is P when $m = a$ (Fig. 10):

$$Load(m) = P \langle x - a \rangle^{-1} N. \tag{39}$$

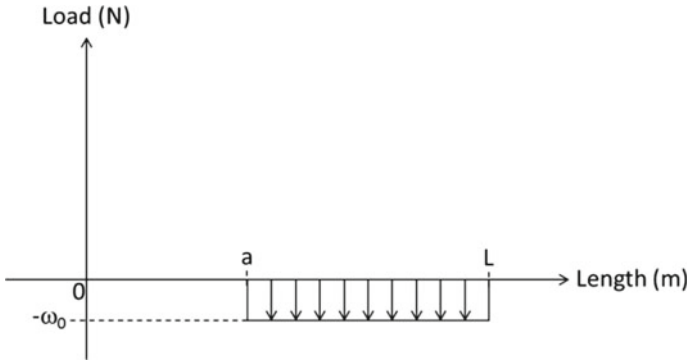


Fig. 8 Constant loading.

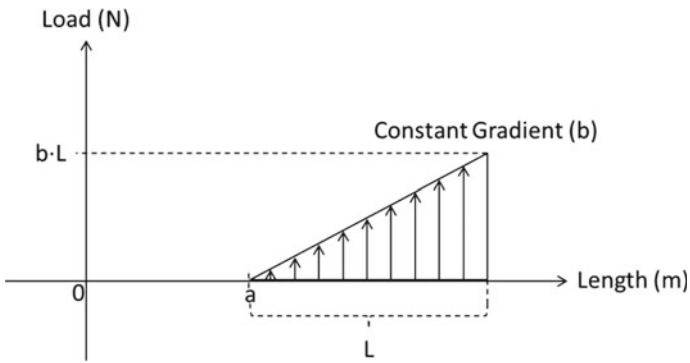


Fig. 9 Linear loading.

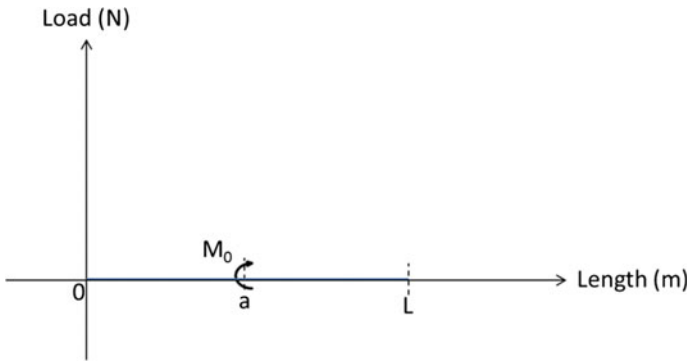


Fig. 10 Moment loading.

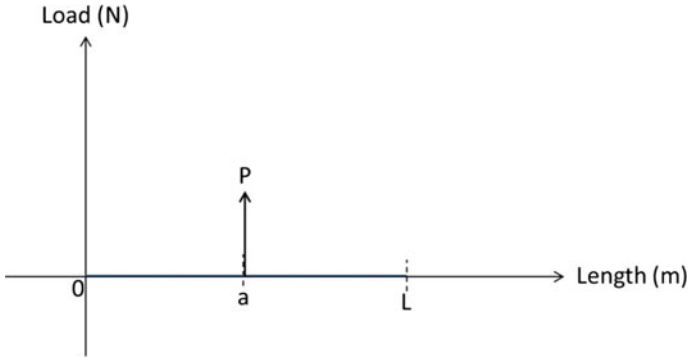


Fig. 11 Impulse loading.

Using free-body diagrams, the load and reaction forces at supports are defined along the length of the rod. The loads(m) are integrated twice to obtain M which is solved for Eq.(30) and is integrated twice again to find the deflection (Fig. 11).

For a magnetic tip experiencing magnetic forces and torques (bending moments),

$$q(x) = \iint F \langle x - a \rangle^{-1} N + M \langle x - a \rangle^{-2} Nm^{-1}. \tag{40}$$

This is solved by applying techniques discussed above to determine the deflection from the applied magnetic torques and forces. Additional boundary information such as bending strain can also be considered depending on the requirements.

4.4 Other Applications of Magnetic Tip Actuation

Other than guide wires and catheters, the magnetic navigations of drill, balloon and needles have also been recommended for a wide variety of surgical needs (Table 2).

5 Theory to Prototype

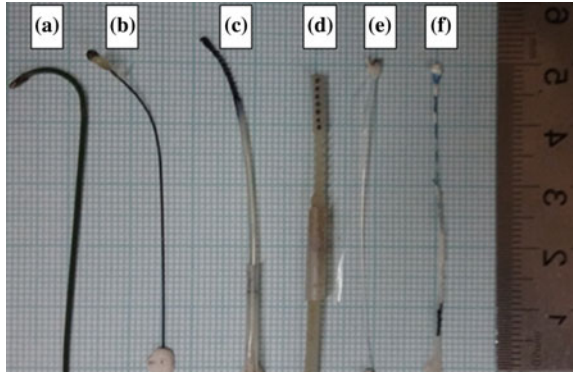
Based on the theory covered in Sects. 4.2 and 4.3, a wide variety of magnetic manipulators (Fig. 12) can be designed, tested and modelled. In the Fig. 12,

- A & B are guide wires with an attached magnetic head.
- C & D are 3D printed design which can be further modified to include a magnetic tip.
- D has multiple magnetic segments.
- E & F are nylon wires with a magnetic tip glued on top.

Table 2 A list of existing applications using magnetic tip actuation.

Surgical/Clinical application	Source
Cardiac ablation	StereoTaxis has developed magnetic catheters for cardiac ablation [6, 8, 10, 13, 43, 46]. By attaching multiple magnetics, the catheter has additional DOFs which allows for more redundancy in actuation. This directly translates to additional positioning of the catheter which is important for cardiac ablation where the heart is still beating and the tip of the catheter has to pulse back and forth in tandem. Stereotaxis has been implemented in a clinical setting [12, 16, 29, 52]
Nasobiliary tube	Placement of a magnetic catheter in a similar fashion [50] to above but for the Gastrointestinal tract
Guide wire control	US20070032746 [38]. A continuous magnetic strip is wrapped around the length of the guide wire for actuation. Such an approach allows for a customizable selection of magnetic elements along the guide wire to tune the magnetic response to various surgical needs
Deep Brain Stimulation electrode implant	Magnetic field is used to guide the insertion of the needle into the deep regions of the brain [36]. The stators utilized here are upscaled versions of OctoMag and the actuators (permanent NdFeB magnets) are hinge supported allowing independent rotation relative to the base. Nitinol wires used to provide translational information while remaining compliant to bending along curvatures. The region of interest is currently 10cm by 10cm. Magnetics could also be used to assist needle puncture, making the procedure safer [39]
Angioplasty	A magnetic attachment to surgical balloons for positioning of the stent or balloon during angioplasty [44]
Stenting	Combining guide wire navigation with stenting allows the navigation of the stent to be directly guided to the target location [49]
Alignment of devices	Magnetics could also be used to connect to catheters together in-vivo to create a continuous delivery line. Without the aid of magnetics, this would be a tedious and arduous task for the surgeon to perform in the patient [9]
Drilling	Precise Steering and Unclogging Motions of a Catheter With a Rotary Magnetic Drill Tip Actuated by a Magnetic Navigation System [21]
Drilling and Stenting	Utilizing precession and rotations in magnetic fields, both drilling and release of a sheathed stent are shown [27]
Micro-endoscope	A magnetic ferrofluid suspension rotor is used to turn a small mirror for micro-endoscopy applications [5]

Fig. 12 Flexible manipulators.



5.1 Test Phantom (F)

The outer diameter of the guide wires and nylon wire were similar, 0.35 mm, but the nylon wire is much more flexible than the guide wire. To make the distal region stiffer, we used a polymer (polycaprolactone) coating via immersion coating; equivalently an external catheter which is more ridged can encase the nylon wire. This will constrict the flexible deflection length to about 20 mm. The magnetic attachments are based on polycaprolactone as the adhesive. The attachment can be much more developed and we cover some ideas in the next section. The size of the attached magnetic component should be similar size to the GW itself; in our case fabrication limitations have left it into a cube of $1 \pm 0.5 \text{ mm}^3$. There is a trade-off if the attached magnetic component is too small; the magnetic dipole moment from the dipole will be weak and may have to be compensated by increasing the external magnetic fluxes from the stators.

5.2 3D Printed Designs (C and D)

Given cross-sectional area limitations, we propose two alternative methods to overcome this via 3D rapid prototyping with flexible material, based on the stratasys Objet260 Connex3 and TangoGray FLX950. The idea is to create allowance for magnetic components along the axis of the manipulator such that the summation of forces and torques will be able to compensate the individually small magnetic moments. Additionally, the benefit of 3D printing comes in when the user wants to customize the design. For example, the distances between the magnetic components and the flexible regions can be rearranged to create unique compositions which can cater to the various medical needs (Fig. 13).

A simple model of guide wire will consist of three portions. The relatively ridged rod transmits axial translation forces from the proximal to the distal end. Since the dimensions are usually fixed, the material choice is the key parameter to deciding its

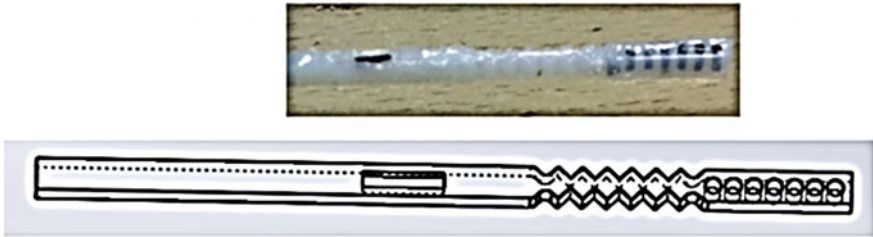


Fig. 13 Flexible manipulator D.

flexibility; notable choices are titanium and steel for small diameters. The sequential segment is the flexible region and defines the bending length. This design removes excess material to induce flexibility relative to the distal end, enhancing bending at this region. Attached to the tip of the flexible region is the magnetically controlled region. This region translates information from the external electromagnetic coils for tetherless actuation. The attachment could come in many forms; here holes for small cylindrical magnets are designed.

There are many methods for magnetic incorporation into the material. Other than a ridged magnetic material, magnetic powder and liquid are also possible means to make a manipulator magnetically responsive. While a simple adhesive solution is possible for ridged permanent magnets, some design may require more sophisticated methods. In extension to the adhesive method, the adhesive can be contained.

Polycaprolactone, a thermo-polymer can be stored in a predefined volume. It is contained in the volume by surface tension and upon heating (water bath); above transition temperature, the guide wire can be inserted into the cavity and the polymer is cooled again to lock the guide wire in place (Fig. 14).

A mechanical tight fit design may also be an option to attaching a magnetic component. In Fig. 15, the threads hold the pieces in place and as it is pushed into the tapered hole. Many other variants are possible with this concept and it is also

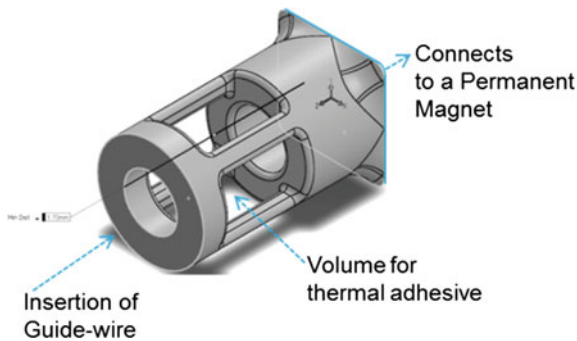


Fig. 14 Connector design for adhesive attachment.

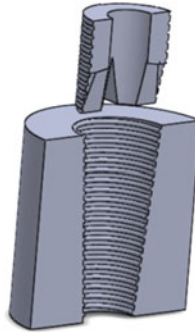


Fig. 15 Connector design for mechanical attachment.

applicable to other fields, such as the luer-lock design. The concept of modular attachment can be beneficial to guide wires which need different types of magnetic attachments. It is also beneficial to the integration of electromagnetic devices into the clinical setting where guide wires are already existent and it is not necessary to custom design a guide wire with the electromagnetic coils. Physicians need only to attach the magnetic tip for magnetic control when needed.

5.3 Control Electronics

Additionally, electronics should be utilized for control such as an Arduino environment. A microcontroller receives joystick bending and translates it into coil currents; refer to Fig. 16 for electronic control. Feedback should also be incorporated for closed-loop control.

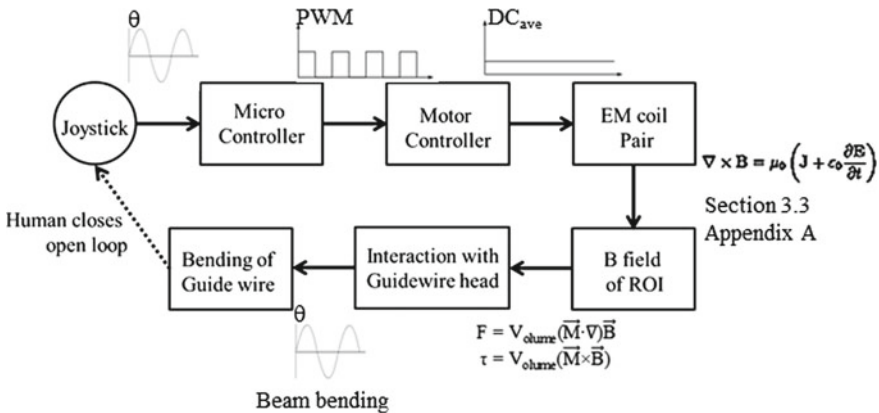


Fig. 16 Information flow of the control electronics.

A joystick or buttons can be used to register user input as an electrical signal. This signal is read by a microcontroller (such as Arduino) and converts the signal into a PWM wave form. PWMs capture the analogue information as a percentage of the duty cycle. A motor controller unit (e.g. L298N) perceives the PWM signal and outputs a DC signal which is an amplification of the initial joystick signal. The motor control unit also defines the maximum voltages and hence the maximum currents. The potential differences across the electromagnetic coils drive a current and by ampere circuital law this generates magnetic fields. The magnetic potentials and gradients in the region of interest interact with the magnetic tip, giving rise to controllable mechanical deflection.

6 Classification of Guide Wire Model

While there are many important parameters to guide wires, we focus here on the bending angle. The bending angle is an important aspect which indicates the type of vessels/blockages it can navigate. We show here a Bézier curve reconstruction to obtain the bending angles. The Bézier curve uses points along the curve to reconstruct the parametric model.

6.1 *Bending Angle*

To obtain our points, we use colour-coded images (Fig. 17a) to define the centroids (Fig. 17b) along the path of the guide wire. The red line shows the reconstructed curve (Fig. 17). As this is a reconstruction using imaging, errors propagating from any of the processes along the work flow will contribute to some degree of error. These errors can be minimized by using more points along the curve especially at regions when the curvature is high. For guide wire applications, the deflection is relatively small and the bending radius is usually large across the length of deflections, and thus errors perceived do not affect the conclusions drawn significantly. The colour codes translate to cells which break the continuous manipulator into smaller segments.

To locate the centroid, processing software (such as MATLAB) is recommended as it has pre-built functions to handle image processing. The mean/medians of each segment is perceived as a histogram on the X/Y axis and is taken to be the centre. A Bézier function takes in the coordinates of each point in order of progression from base to tip. Each point is connected to subsequent points forming the first-order line. A number of the parametric intervals are then selected. This number represents the segmentation between points on the first-order line, and more parametric point will mean a smooth curve at the cost of computational power. Points on the first-order line corresponding to the parametric integer build the second-order line. The line-forming process is nested until no further lines can be built. On the final-order line, the point corresponding to the parametric integer represents the Bézier curve's value

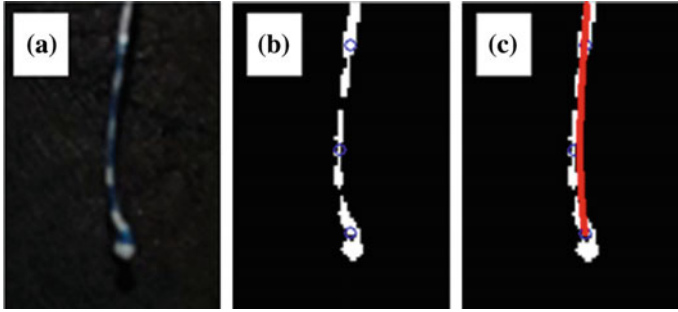


Fig. 17 The image processing for curve reconstruction.

at that parametric integer. The Bézier curve allows a continuous connection between the first and last coordinates, and allows us to interpolate and estimate coordinates for the entire curve.

The bending angle can be taken at any point along the Bézier curve. Here, we compare between the start and end of the curve. Given a joystick input (Fig. 18), we can get bending angles (Fig. 19) and the reconstructed curves at time points of interest (Fig. 20). Other notable parameters that are also extractable are the radius of curvature.

7 System Experiment

In the surgical context, the bending angles achieved can navigate obstacles such as stenosis.

Figure 21 a Upon encounter of an obstacle, the bending angle can create different paths for advancement (Fig. 21b, c), and post-selection of path the guide wire can be

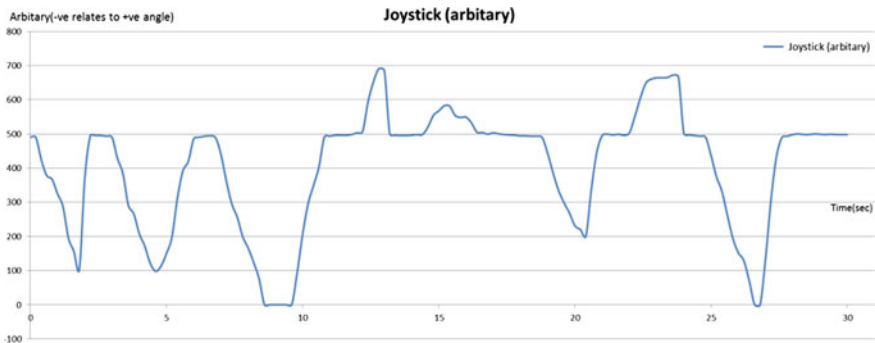


Fig. 18 Input from joystick.

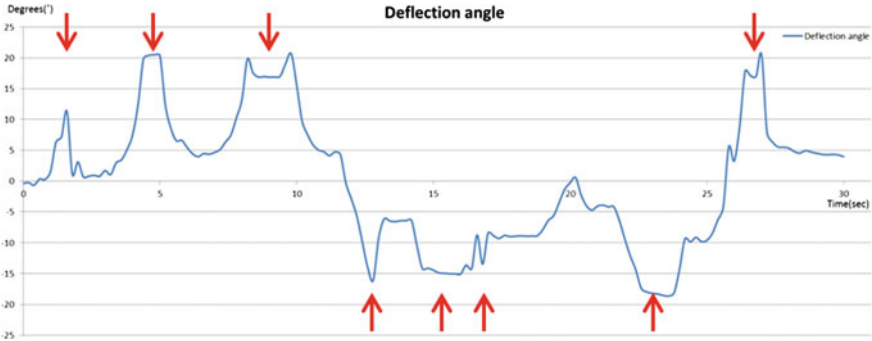


Fig. 19 Output in bending angles.

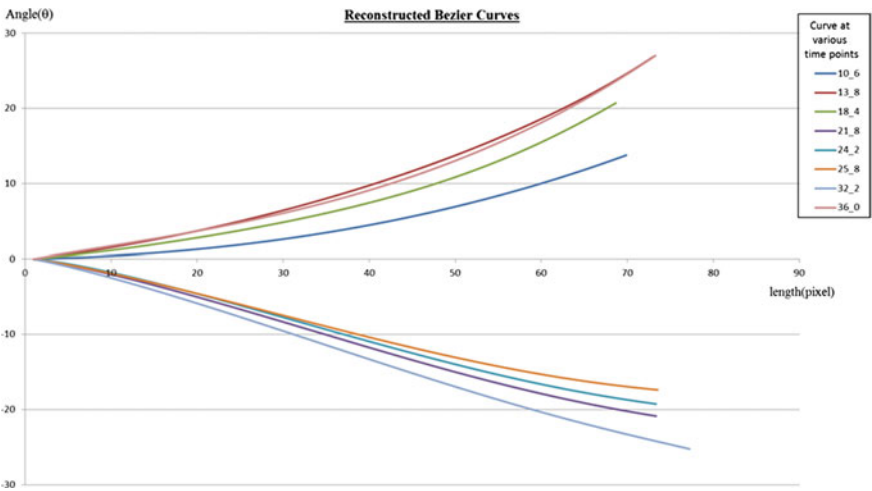


Fig. 20 Bezier curve reconstructions.

advanced to bypass the obstacle (Fig. 21d). In more realistic scenarios, the vision of the operator may be impaired and the actual deflection for advancement is not known. Thus, the operator would constantly sweep through different bending angles at the site to test for advancement; obstruction is detected either through angiography or through ultrasound of tactile information. The deflection shown here is translatable, although to a lesser extent, to more ridged guide wires.

Figure 22b indicates the neutral position of the guide wire. The guide wire is pre-curved and can preferentially bend in one direction (more compliant), while extension in the opposite direction is much more ridged. Compliant bending by electromagnetic interaction is shown in Fig. 22a and extension/straightening of the guide wire is shown in Fig. 22c. As the bending angles are rather small due to the stiffness of the guide wire, Fig. 22a, b and c is superimposed in Fig. 22d. The rigidity in straightening the guide wire is also visible by comparing deflections between Fig. 22a and c. A stronger

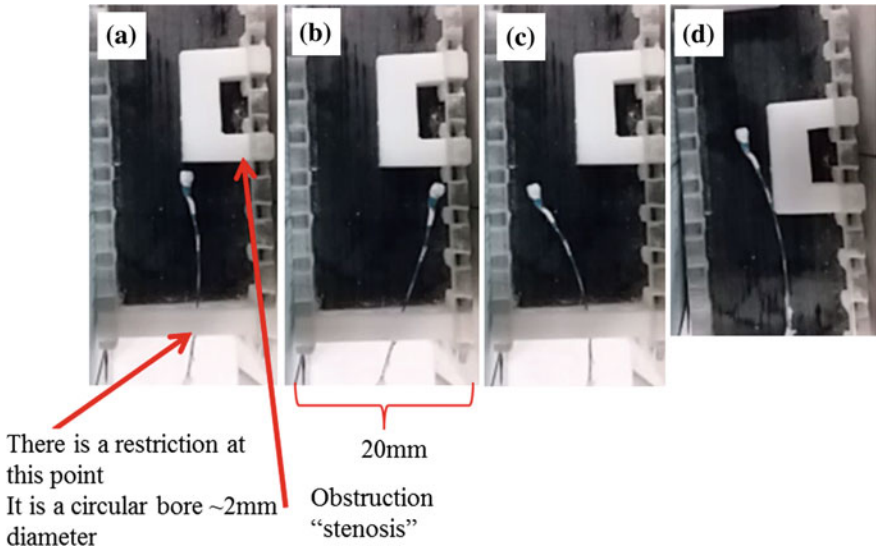


Fig. 21 Prototype navigating a modelled environment.

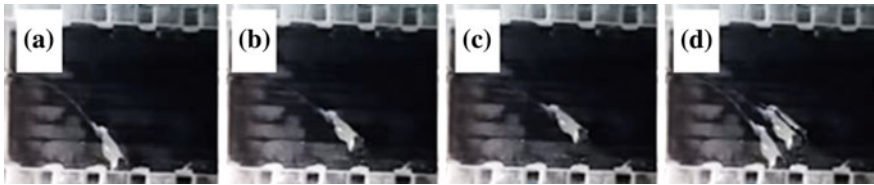


Fig. 22 Guide wire deflection.

magnetic field generated will allow further deflection angles but the concept shown here will allow physicians to direct control over the distal tip which was previously not possible. The reliance on buckling of the guide wire from traditional methods is removed along with the associated risk and uncertainties.

8 Conclusions and Future Direction

Manipulator-based surgical equipment generally suffers from mechanical disturbance during operation and this chapter has illustrated the electromagnetic approach to improve controllability over the distal end. Improving distal end control such as in guide wires for surgical procedures can improve treatment options (angioplasty). The use of untethered electromagnetic interactions consists of two main parts: the actuator and the stator. There are many ways to design and construct the system but ultimately the end goal is to achieve a controllable deflection/bending angle to nav-

igate obstacle and overcome distal mechanical control limitations. We have further shown in this chapter a method to achieve such a system with a simple magnetic tip attachment. From the base design, more complicated features can be added to cater for various needs. From a design stand point, the introduction of electromagnetic control should reduce the mechanical complexity of the procedure. To illustrate, an electromagnetic guide wire can replace a wide range (with different curvatures and bending angles) of guide wire each catering to a specific anatomical region. Therefore, one should consider electromagnetic manipulation as beneficial to distal control and additionally can impact integration at a low-cost implementation.

While electromagnetics provides a good means to actuate, the need for closed-loop control in stability is not covered in this chapter. Present imaging modalities include MRI, NIR and ultrasounds. The acoustic or optical images should be extracted for features to perform real-time tracking such that automation can be achieved. The system which is electromagnetically driven could, in theory, also be used for sensing and position guidance. The domain of transducers and integration with external imaging systems should not be overlooked. The incorporation of electromagnetic sensing capabilities can be achieved with Hall effect sensors, flex sensor, or even inductor-based sensors. However, considering that the use of ultrasound is well established, incorporation of an Ultrasonic system for automated guidance and delivery of guide wire is likely to be the direction in the near future.

8.1 Electromagnetic Actuation in PAD: Future Directions

A notable limitation in current magnetic navigation systems is the use of the external magnetic field generators which are rather bulky in size in order to generate the 0.1–0.15 Tesla fields. Thus if possible the external generators implemented should not increase the bulk of the design to the point where it obstructs movement or vision of the patient or the physician. In an idealized case, the external generators should be eliminated completely and reduce the bulk of the system; this would be favourable in saving the theatre space required to do the procedure.

Present catheters (4 mm) used are also much larger than guide wires (1 mm) and there exists a challenge to minimize the design. However, the magnetic guidance systems were documented to be effective on micro-robots (less than 1 mm), and thus it should be viable for a guide wire design to be magnetically manipulated. There exists a gap in the current implementations for magnetically manipulated guide wires for where there are more stringent requirements on the guide wires as the arteries are much small in the distal positions of the peripherals limbs. Present implementations are focused on the applications in the heart and the brain.

Implementation for the magnetic manipulation poses a viable option for PAD as the magnetic fields to not harm the body and allows for contactless transmission of force/control through human tissue. A concern could exist where the imaging X-rays (CT) or MR imaging could interfere with control of the guide wire, but as Sterotaxis Epoch system is an implemented device, this should be a trivial issue.

An additional note is that current guide wire systems have only used imaging techniques for position sensing, and thus it may be prudent to include force sensing capabilities such as those used in calcific iliac occlusion devices TruePath™ to provide haptic/tactile feedback to the surgeons. Further, while there have been many approaches for magnetic guide wire design, none of them has been tested for implementation for PAD. Thus, there exists a need to design a specific system catered for PAD.

Acknowledgements This work is supported by the Singapore Academic Research Fund under Grant R-397-000-173-133, NUSRI China Jiangsu Provincial Grant BK20150386 & BE2016077 awarded to Dr. Hongliang Ren.

References

1. Aalami, Oliver, et al. 2015. Prevention of Juxta-Anastomotic AV Fistula Stenosis With Implantation of an ePTFE Covered Endograft at Time of AV Fistula Creation. *Journal of Vascular Surgery* 61 (6): 101–102S.
2. J.J. Abbott et al. 2007. Modeling Magnetic Torque and Force for Controlled Manipulation of Soft-Magnetic Bodies. In *IEEE Transactions on Robotics* 23.6, pp. 1247–1252. ISSN: 1552-3098. <https://doi.org/10.1109/TRO.2007.910775>.
3. Abbott, Jake J., et al. 2009. How Should Microrobots Swim? English. *The International Journal of Robotics Research* 28 (11–12): 1434–1447.
4. Afshin Anssari-Benam, Dan L. Bader, and Hazel R. C. Screen. 2011. A combined experimental and modelling approach to aortic valve viscoelasticity tensile deformation. *Journal of Materials Science: Materials in Medicine* 22.2, pp. 253–262.
5. Assadsangabi, Babak, et al. 2016. Catheter-based microrotary motor enabled by Ferrofluid for microendoscope applications. *Journal of Microelectromechanical Systems* 25 (3): 542–548.
6. Bauernfeind, Tamas, et al. 2011. The magnetic navigation system allows safety and high efficacy for ablation of arrhythmias. *Europace* 13 (7): 1015–1021.
7. Bouchebout, Soukeyna, et al. 2012. An overview of multiple DoF magnetic actuated microrobots. *Journal of Micro-Nano Mechatronics* 7 (4): 97–113.
8. Jason Bradfield et al. 2012. Catheter ablation utilizing remote magnetic navigation: a review of applications and outcomes. *Pacing and Clinical Electrophysiology* 35 (8): 1021–1034.
9. William D.F Christopher P.S. 2010. *U.S. Patent No.2012,0,089,089*. en. Washington, DC: U.S. Patent and Trademark Office.
10. Julian K. Chun et al. 2007. Remote-controlled catheter ablation of accessory pathways: results from the magnetic laboratory. *European Heart Journal* 28.2, pp. 190–195.
11. Dember, Laura M., et al. 2005. Design of the dialysis access consortium (DAC) clopidogrel prevention of early AV fistula thrombosis trial. *Clinical Trials* 2 (5): 413–422.
12. Ernst, Sabine, et al. 2004. Initial experience with remote catheter ablation using a novel magnetic navigation system: magnetic remote catheter ablation. *Circulation* 109 (12): 1472–1475.
13. Faddis, Mitchell N., and Bruce D. Lindsay. 2003. Magnetic catheter manipulation. *Coronary Artery Disease* 14 (1): 25–27.
14. F.G.R. Fowkes et al. 2013. Comparison of global estimates of prevalence and risk factors for peripheral artery disease in 2000 and 2010: a systematic review and analysis. *Lancet (London, England)* 382.9901, pp. 1329–1340.
15. Anna Franzone et al. 2012. The role of atherectomy in the treatment of lower extremity peripheral artery disease. *BMC surgery* 12 Suppl 1. Suppl 1, S13–S13.

16. Haghjoo, Majid, et al. 2009. Initial clinical experience with the new irrigated tip magnetic catheter for ablation of scar-related sustained ventricular tachycardia: a small case series. *Journal of Cardiovascular Electrophysiology* 20 (8): 935–939.
17. Hod, Tammy, et al. 2014. Factors predicting failure of AV fistula first policy in the elderly: predictors of AVF failure. *Hemodialysis International* 18 (2): 507–515.
18. Walter H. Hörl et al. 2004. *Replacement of renal function by dialysis*. Fifth / by Walter H. Hörl, Karl M. Koch, Robert M. Lindsay, Claudio Ronco, James F. Winchester (-in-chief).;1; 5th; Dordrecht: Springer Science+Business Media. ISBN: 9781402022753; 1402022751; 9789401570121; 9401570124.
19. Iacovacci, Veronica, et al. 2015. Untethered magnetic millirobot for targeted drug delivery. *Biomedical Microdevices* 17 (3): 1–12.
20. Ahmed A. Al-Jaishi et al. Patency rates of the arteriovenous fistula for hemodialysis: a systematic review and meta-analysis. *American Journal of Kidney Diseases: The Official Journal of the National Kidney Foundation* 63.3 (2014;2013), p. 464.
21. Jeon, S.M., and G.H. Jang. 2012. Precise steering and unclogging motions of a catheter with a rotary magnetic drill tip actuated by a magnetic navigation system. *IEEE Transactions on Magnetics* 48 (11): 4062–4065.
22. Jeon, Seungmun, et al. 2010. Magnetic navigation system with gradient and uniform saddle coils for the wireless manipulation of micro-robots in human blood vessels. *IEEE Transactions on Magnetics* 46 (6): 1943–1946.
23. Jeong, Semi, et al. 2011. Enhanced locomotive and drilling microrobot using precessional and gradient magnetic field. *Sensors and Actuators A: Physical* 171 (2): 429.
24. K. Konner. 2003. Vascular access in the hemodialysis patient personal experience and review of the literature. en. In *Hemodialysis International* 7.2, pp. 184–190. <https://doi.org/10.1046/j.1492-7535.2003.00026.x>.
25. Lanzer, P. 2013. *Catheter-Based Cardiovascular Interventions: A Knowledge-based Approach*. New York: Springer.
26. P. Lanzer and Inc Ovid Technologies. *Mastering endovascular techniques: a guide to excellence*. Philadelphia: Lippincott Williams & Wilkins, 2007; 2006; ISBN: 9781582559674; 1582559678.
27. Wonseo Lee et al. 2017. Selective motion control of a crawling magnetic robot system for wireless self-expandable stent delivery in narrowed tubular environments. *IEEE Transactions on Industrial Electronics* 64.2, pp. 1636–1644.
28. Lim, Gregory B. 2013. Peripheral artery disease pandemic. *Nature Reviews Cardiology* 10 (10): 552.
29. Jianhua Liu et al. 2016. Design and fabrication of a catheter magnetic navigation system for cardiac arrhythmias. *IEEE Transactions on Applied Superconductivity* 26.4, pp. 1–4.
30. X. Liu, G.J. Mancini, and J. Tan. 2015. Design and Analysis of a Magnetic Actuated Capsule Camera Robot for Single Incision Laparoscopic Surgery. In *2015 IEEE/RSJ International Conference on Intelligent Robots and Systems (IROS)*, pp. 229–235. <https://doi.org/10.1109/IROS.2015.7353379>.
31. Arthur W. Mahoney and Jake J. Abbott. 2016. Five-degree-of-freedom manipulation of an untethered magnetic device in fluid using a single permanent magnet with application in stomach capsule endoscopy. *The International Journal of Robotics Research* 35.1-3, 129–147.
32. Hamal Marino, Christos Bergeles, and Bradley J. Nelson. 2014. Robust electromagnetic control of microrobots under force and localization uncertainties. *IEEE Transactions on Automation Science and Engineering* 11.1, 310–316.
33. Misakian, M. 2000. Equations for the magnetic field produced by one or more rectangular loops of wire in the same plane. *Journal of research of the National Institute of Standards and Technology* 105 (4): 557.
34. Mukherjee, Debabrata, et al. 2010. *Cardiovascular Catheterization and Intervention: A Textbook of Coronary, Peripheral, and Structural Heart Disease*. Baton Rouge: CRC Press.
35. J.M.S. Pearce. 2009. Henry gray's anatomy. In *Clinical Anatomy* 22.3, pp. 291–295. issn: 1098-2353. <https://doi.org/10.1002/ca.20775>.

36. A. J. Petruska et al. 2016. Magnetic needle guidance for neurosurgery: Initial design and proof of concept. In *2016 IEEE International Conference on Robotics and Automation (ICRA)*, pp. 4392–4397. <https://doi.org/10.1109/ICRA.2016.7487638>.
37. Peter Schneider. *Endovascular skills : guidewire and catheter skills for endovascular surgery*. 3rd ed. CRC Press, 2009;2008; ISBN: 1420069373; 9781420069372.
38. J.C. Sell. 2007. *U.S. Patent No. 2007,0,032,746*. Washington, DC.
39. J.C. Sell. 2005. *U.S. Patent No. 8,419,681*. Washington, DC: U.S. Patent and Trademark Office.
40. S. Song, H. Yu, and H. Ren. 2015. Study on mathematic magnetic field model of rectangular coils for magnetic actuation. In *2015 IEEE 28th Canadian Conference on Electrical and Computer Engineering (CCECE)*, pp. 19–24. <https://doi.org/10.1109/CCECE.2015.7129153>.
41. Studies from Swiss Federal Institute of Technology Have Provided New Information about Nanoparticles. In *Nanotechnology Weekly* (2012), p. 352.
42. Subramaniam, Tavintharan, et al. 2011. Distribution of ankle-brachial index and the risk factors of peripheral artery disease in a multi-ethnic Asian population. *Vascular Medicine* 16 (2): 87–95.
43. Tamas Szili-torok et al. 2012. Catheter ablation of ventricular tachycardias using remote magnetic navigation: a consecutive case-control study. *Journal of Cardiovascular Electrophysiology* 23 (9): 948–954.
44. Libo Tang, Yonghua Chen, and Xuejian He. 2007. Magnetic force aided compliant needle navigation and needle performance analysis. IEEE, pp. 612–616. ISBN: 1424417619; 9781424417612; 9781424417582; 1424417589.
45. TDK Europe – *EPCOS - Material Data Sheets*.
46. A.S. Thornton et al. 2006. Magnetic navigation in AV nodal re-entrant tachycardia study: early results of ablation with one- and three-magnet catheters. In *Europace : European Pacing, Arrhythmias, and Cardiac Electrophysiology: Journal of the Working Groups on Cardiac Pacing, Arrhythmias, and Cardiac Cellular Electrophysiology of the European Society of Cardiology* 8.4, pp. 225–230.
47. I. Tunay. 2004. Modeling magnetic catheters in external fields, vol. 1. IEEE, pp. 2006–2009. ISBN: 9780780384392; 0780384393.
48. I. Tunay. 2004. Position control of catheters using magnetic fields. In IEEE, pp. 392–397. ISBN: 0780385993; 9780780385993;
49. J.C Viswanathan R.R. and Sell. 2006. *U.S. Patent No.8,348,858*. Washington, DC: U.S. Patent and Trademark Office.
50. Watanabe, Seitaro, et al. 2013. Positioning of nasobiliary tube using magnetloaded catheters. *Endoscopy* 45 (10): 835–837.
51. J.E. White et al. 2012. Development of a lorentz-force actuated intravitreal jet injector. In IEEE, pp. 984–987. ISBN: 1557-170X.
52. Mark, A. Wood, et al. 2008. Remote magnetic versus manual catheter navigation for ablation of supraventricular tachycardias: a randomized, multicenter trial. *Pacing and Clinical Electrophysiology* 31 (10): 1313–1321.
53. Wu, Cong C., et al. 2015. The outcome of the proximal radial artery arteriovenous fistula. *Journal of Vascular Surgery* 61 (3): 802–808.
54. Steven Wu and Sanjeeva P. Kalva. 2015. *Dialysis Access Management*. Cham: Springer International Publishing. ISBN: 3319090933; 9783319090931; 9783319090924; 3319090925.
55. Zhou, H., J. Sun, B.S. Yeow, H. Ren 2016. Multi-objective parameter optimization design of a magnetically actuated intravitreal injection device. In IEEE 14th International Workshop on Advanced Motion Control (AMC). *Auckland, New: Zealand* 2016: 430–435. <https://doi.org/10.1109/AMC.2016.7496388>.